Experimental validation of two-dimensional displacement measurement of string vibration through optical model*

☆ Tomoya Niimi, Natsuki Yoshino, Kohei Yatabe (Tokyo University of Agriculture and Technology)

1 Introduction

String vibration of musical instruments exhibits two-dimensional motion depending on excitation conditions such as bowing and plucking. Measuring this motion is essential for understanding sound production and acoustic characteristics of musical instruments. We have previously proposed a non-contact method for measuring two-dimensional string vibration using a single high-speed camera and a defocusing technique [1]. In this method, two-dimensional string vibration is measured by tracking the position of the intensity peak in the defocused image, while the intensity distribution itself strongly depends on the imaging settings. To characterize this dependence, we developed an optical model based on geometrical optics and validated it through comparison with observed images [2]. The Gaussian-filter parameters in [1] have been empirically chosen under different imaging conditions. This empirical choice does not provide a systematic criterion for selecting suitable parameters for each setting. In this study, to address this, we use the optical model presented in [2] to quantitatively investigate the Gaussian-filter parameters under several conditions, with the aim of improving string displacement estimation.

2 Measurement method

The coordinate system used in the defocusing measurement method [1] is shown in Fig. 1. The method uses a single high-speed camera equipped with a large-aperture lens, where the camera is positioned at a low elevation angle relative to the string. As shown in Fig. 2, when the lens aperture is widened to create a shallow depth of field, the image of the string away from the focal plane is blurred, whereas the region near the focal plane is observed as a localized bright region. In each frame, the position of the bright intensity peak is detected. The vibration of the string is then tracked by comparing the peak position in each frame with the static peak position. The two-dimensional displacement of a point on the string is obtained from the difference between these positions. To improve displacement-estimation accuracy, a two-dimensional quadratic surface is fitted to the intensity values around the peak pixel, and the maximum of the fitted surface is used to estimate the peak position with subpixel precision.

In this study, observed images are compared with simulated images generated using the optical model proposed in [2]. Let $(\tilde{u}, \tilde{v})$ denote the coordinates on the image plane, D be the effective aperture diameter of the lens, a_0 be the object distance to the reference point on the string, b_0 be the corresponding image distance, Φ be the string diameter, and θ be the elevation angle between the camera and the string. The standard deviation $s(\tilde{v})$, which represents the spread of the observed intensity distribution in the $\tilde{u}$ direction, is given by

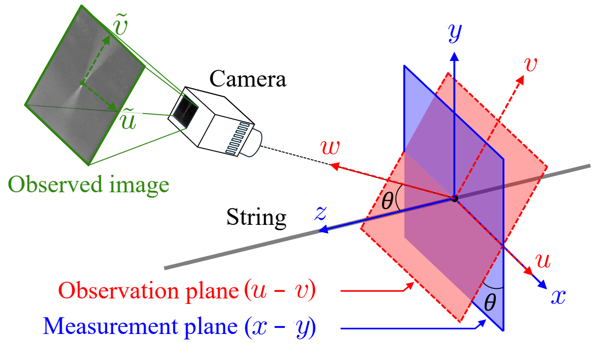

Fig. 1 Coordinate system used in the proposed measurement method.

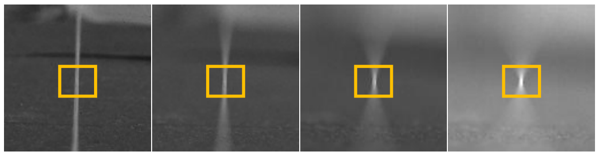

Fig. 2 Observed images of a string obtained with different aperture settings. From left to right, the lens aperture is widened. The yellow square marks the region near the focal plane.

$$s(\tilde{v}) = \frac{1}{4}\sqrt{\left(\frac{D\,|\tilde{v}|}{a_0 \tan\theta}\right)^2 + \left(\frac{b_0}{a_0}\Phi\right)^2}. \qquad (1)$$

The normalized intensity distribution is then expressed as

$$I(\tilde{u}, \tilde{v}) = \frac{1}{\sqrt{2\pi}\, s(\tilde{v})} \exp\left(-\frac{\tilde{u}^2}{2 s(\tilde{v})^2}\right). \qquad (2)$$

Equation (1) indicates that a smaller elevation angle θ leads to a larger deviation in the width of the defocused image with respect to the position in the $\tilde{v}$ direction. This model is used to simulate the spatial intensity distribution of the defocused image and to determine the image-processing and experimental conditions based on the simulation results.

3 Experiments

Under practical imaging conditions, shot noise causes fluctuations in the detected intensity-peak position and degrades displacement-estimation precision. To investigate this effect, defocused images with prescribed peak positions were generated using the optical model, and Poisson-distributed shot noise was added to the generated images. Two numerical experiments were conducted: the Gaussian-

*弦振動二次元変位計測における光学モデルに基づく計測条件の検証. 新美智也, 吉野夏樹, 矢田部浩平 (農工大).

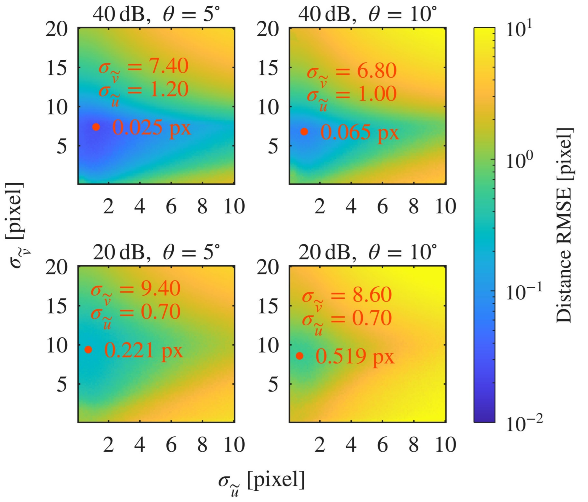

Fig. 3 Heat maps of the peak localization error evaluated on simulated images over the $(\sigma_{\tilde{u}}, \sigma_{\tilde{v}})$ parameter space. Red markers indicate the minimum RMSE under each condition.

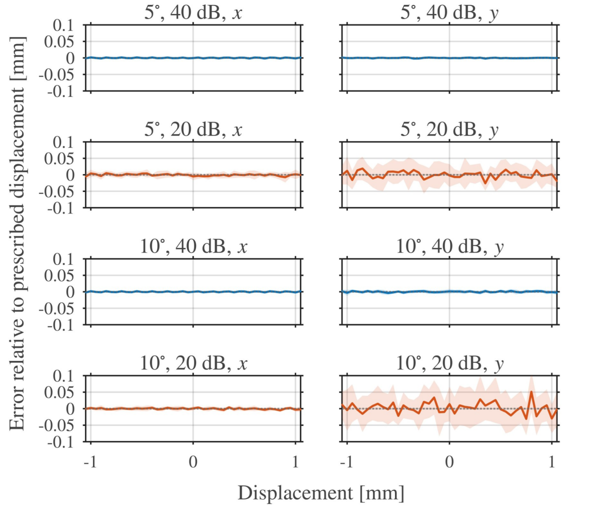

Fig. 4 Mean displacement-estimation errors and standard deviations as functions of the prescribed displacement.

filter parameters were first selected for each combination of an elevation angle and the SNR, and the displacement-estimation errors were then evaluated using prescribed displacements and the selected parameters. The physical parameters were set to $D = 25.0\,\mathrm{mm}$, $a_0 = 220\,\mathrm{mm}$, $b_0 = 41.5\,\mathrm{mm}$, and $\Phi = 0.660\,\mathrm{mm}$. The elevation angle was set to $\theta = 5°$ or $10°$, and the SNR was set to 20 dB or 40 dB. The image size was fixed at 128×128 pixels. Under these conditions, the image scale on the measurement plane was 0.147 mm per pixel.

3.1 Selection of noise-reduction parameters

Before peak detection, anisotropic Gaussian smoothing was applied with standard deviations $\sigma_{\tilde{u}}$ and $\sigma_{\tilde{v}}$ in the image-plane directions. A local two-dimensional Gaussian was fitted by regression to a 5×5 pixel region centered at the peak pixel. Ten peak positions were randomly assigned within the image. For each filter-parameter pair $(\sigma_{\tilde{u}}, \sigma_{\tilde{v}})$, a normalized defocused image was generated at each peak position. To model shot noise in actual imaging, Poisson-distributed noise was independently generated and added 10 times to each image, yielding 100 trials in total. The RMSE between the estimated and true peak positions was then calculated over all valid trials.

Fig. 3 shows heat maps of the RMSE over the evaluated $(\sigma_{\tilde{u}}, \sigma_{\tilde{v}})$ parameter space. The minimum RMSE was achieved in regions where $\sigma_{\tilde{v}} > \sigma_{\tilde{u}}$ under all conditions. This result indicates that stronger smoothing along the $\tilde{v}$ direction is effective for defocused images with the elongated shape shown in Fig. 2. The minimum RMSE ranged from 0.025 to 0.519 pixels over the evaluated conditions. The parameter values obtained from this evaluation were used in the following displacement-estimation error evaluation.

3.2 Uncertainty assessment

To evaluate the displacement-estimation performance using the selected Gaussian-filter parameters, simulated defocused images were generated at prescribed positions corresponding to horizontal or vertical displacements from the initial position. The prescribed displacement ranged from $-1.0\,\mathrm{mm}$ to $1.0\,\mathrm{mm}$ in increments of 0.05 mm in each direction. For each prescribed displacement, 10 noisy images were independently generated by adding Poisson-distributed noise corresponding to an SNR of 20 dB or 40 dB, and the peak position was estimated after Gaussian filtering. The displacement-estimation error was defined as the estimated displacement minus the prescribed displacement.

Fig. 4 shows the measurement error under each condition. The solid lines represent the mean displacement-estimation errors, and the shaded regions indicate the standard deviation from the mean. At an elevation angle of 10°, the RMSE ranged from 1.35 µm to 5.27 µm under the 40 dB SNR condition and from 6.06 µm to 51.04 µm under the 20 dB SNR condition. The error tended to be larger in the vertical direction than in the horizontal direction. This tendency may be attributed to the direction-dependent width of the observed intensity distribution, which affects the sensitivity of subpixel localization.

4 Conclusion

This study experimentally evaluated the defocus measurement method under conditions selected based on an optical model. Future work will examine perspective-projection effects associated with the camera elevation angle and validate the method under dynamic string-vibration conditions.

References

[1] T. Niimi, M. Ando, K. Yamada and K. Yatabe, "Measurement of electric guitar string vibration by high-speed camera and estimation of pickup output (in Japanese)," *Proc. Autumn Meet. Acoust. Soc. Jpn.*, pp. 1303–1304 (2024.9).

[2] T. Niimi and K. Yatabe, "Optical model for two-dimensional displacement measurement of string vibration by defocusing (in Japanese)," *Proc. Spring Meet. Acoust. Soc. Jpn.*, pp. 1239–1240 (2026.3).